Numerical Simulation of Microstamping Process to Fabricate Multi-channel of SUS304 Thin Sheets with Consideration of Grain Structures

Shangyu Si
Qiong Wu
Deqing Mei
Wenze Mao
Shufan Song
Liming Xu
Tao Zuo
Yancheng Wang (yanchwang@zju.edu.cn)
Zhejiang University https://orcid.org/0000-0001-5231-6283

Research Article

Keywords: Microstamping, Size effects, Sheet forming, Constitutive model. Springback

Posted Date: March 18th, 2022

DOI: https://doi.org/10.21203/rs.3.rs-1448223/v1

Numerical Simulation of Microstamping Process to Fabricate Multi-channel of SUS304 Thin Sheets with Consideration of Grain Structures

Shangyu Si[a], Qiong Wu[b], Deqing Mei[a,b], Wenze Mao[b], Shufan Song[c], Liming Xu[c], Tao Zuo[c], Yancheng Wang[a,b]*

[a]*State Key Lab of Fluid Power and Mechatronic Systems, School of Mechanical Engineering, Zhejiang University, Hangzhou 310027, China*
[b]*Key Laboratory of Advanced Manufacturing Technology of Zhejiang Province, School of Mechanical Engineering, Zhejiang University, Hangzhou 310027, China*
[c]*Edelman hydrogen energy equipment Co., Ltd, Jiaxing, China*
**Corresponding author: Yancheng Wang, E-mail: yanchwang@zju.edu.cn*

Abstract:

The springback behavior of thin metal sheets will significantly affect the forming accuracy of microchannels during microstamping process, especially as the forming scale reduced to micro/meso levels due to the size effects and grain structures. This paper aims to study the size effects on springback behavior and microchannel's formability in microstamping process. The thin sheet of SUS304 specimens with different grain sizes were prepared and employed in uniaxial tensile tests to examine the stress-strain relationship and used to study the effects of grain sizes on the material's plastic deformation behavior. A constitutive model incorporate surface layer and grain structures is developed to characterize the deformation behavior of thin-metal sheet with different grain sizes. Then, the constitutive model is utilized in finite element simulation of microstamping process to fabricate microchannel structures, and the results are verified by experimental testing. Both numerical simulation and experimental results showed that the size effect is critical in microstamping process, the developed constitutive model is able to accurately characterize the global springback behavior of thin metal sheets during microstamping process.

Keywords: Microstamping; Size effects; Sheet forming; Constitutive model; Springback.

1 Introduction

With the development of machinery industry, miniaturized products and devices have been widely utilized in microelectronic components and medical devices due to their small size, light weight, low cost, and low energy consumption [1]. Several manufacturing processes have been proposed to fabricate these miniaturized structures and devices. Micro-forming has the advantages in high precision and high efficiency, thus regarded as the promising method to fabricate microparts and microstructures [2,3].

In meso/micro-scale forming, the deformation behavior of thin sheet metals will be greatly affected by size effects. Thus, it would be different from that at macro-scale, and macro-plastic forming theory would be no longer applicable [4,5]. To explain the influences of size effect on the sheet metal micro-forming process, several studies have been conducted. Suzuki et al [6] performed micro-tensile experiments on pure aluminum foils with grain sizes of 48 μm, it is found that the yield strength of the material and the strain hardening coefficient increases with the decreasing of the thickness. Michel et al [7] found that the flow stress of sheets with large thickness decreases slowly with the reducing of sheets' thickness, while the flow stress of sheets with small thickness decreases rapidly. Engel and Eckstein [8] investigated the influences of the grain size of the material on the forming of the brass by extrusion and hardness experiments. They found that the microstructure of the grains will affect the forming quality. Most of the studies on the size effects using the tensile and/or compression tests, the effects of size effect on the formation of microchannels still need to be investigated and become one goal of this research.

In micro-forming, thin sheet metals will exhibit different deformation characteristics than that in macro-scale dimensions [9,10]. Therefore, a constitutive model is generally required to be built and used to describe the material deformation in micro-forming process with the aim to obtain more accurate deformation laws and size effect influence laws. Geiger [11] proposed a surface layer model to explain the phenomenon of size effect, it describes that the confinement of the grains is mainly created by the grain boundaries. All surfaces of the inner grains of material are wrapped by grain boundaries, while the surface grains have free surfaces without grain boundaries. Therefore, for thin sheet metals, the surface grains are constrained

more than that of inner grains. As the proportion of surface grains increase, the flow stress of the material will decrease accordingly. Peng et al. [12] combined the surface layer model with Hall-Petch model to formulate a hybrid constitutive model, the size effect affects the flow stress of the metal during sheet forming process was investigated. Then, Peng et al. [13] established a new constitutive model based on the strain gradient (CMSG) plasticity, and finite element (FE) modeling was conducted to simulate the stamping process to make microchannels. Based on the research results of grain structure, Kim et al. [14] developed a grain boundary model for studying micro-rolling process. Xu et al. [15] proposed an extended coupled damage model based on GTN and Thomason models, which considered the geometric and size effects of the void evolution process. The model was applied to FE simulation, the forming limit prediction curves under different scale factors were constructed. Zhang et al. [16] developed a constitutive model for describing the flow stress affected by the strain path change (SPC) and size effect, which provided a basis to support the multi-stage forming. The surface layer model and grain boundary model may not be accurate enough to describe the deformation behavior of thin sheet metals during microchannels forming process. In this study, both grain size effects and sheet geometric size effect will be analyzed and used to establish a constitutive model to accurately predict the deformation behavior of thin sheet stainless steel for microchannels fabrication.

Based on the proposed constitutive model, FE modeling is usually utilized to numerically simulate the influences of size effect on the deformation behavior [17,18]. Wang et al. [19] utilized the FE modeling to divide the specimen into three parts including free surface, transition and internal parts. Through numerical simulation, the dispersion of the flow stress and non-uniformity of the deformation can be predicted, and the simulation results were in good agreement with experimental tests. Molotnikov et al. [20] used a dislocation constitutive model considering the influence of thickness to simulate the forming process, it was shown that the thickness effects are mainly depends on the ratio of thickness (t) to grain size (D). Lu et al. [21] used Voronoi tessellation to develop a FE model to study the effects of grain size on the deformation behavior of material. Wang et al. [22] established a FE model to simulate micro-bending process based on different grain sizes, the geometric model of the grain structures was constructed by Voronoi tessellation. The results showed that stress concentration

occurs at the grain boundaries of the microparts during micro-bending process. The above studies have not thoroughly investigated the effects of size effects in the fabrication of microchannels, thus FE model needs to be established and to study the microchannels fabrication in microstamping process and become one goal of this research.

From the above review, it can be observed that there are few studies on constitutive models considering both the effects of grain size and sheet geometry. There is still a lack of systematic research on the multi-channel forming behavior of sheets under different grain size conditions. Therefore, this study firstly conducted uniaxial tensile experiments to obtain the plastic behavior of different grain sizes. Then established a hybrid constitutive model that considered the grain size effect and sheet geometry effect, and using FE simulation and multi-channel microstamping experiments to verify the developed constitutive model. The influences of the size effect on the von mises stress distribution and formability of stainless-steel sheets under the conditions of different geometric sizes and grain sizes will be investigated.

2 Tensile Testing of Plastic Deformation Behavior

2.1 Specimen Preparation

Commercialized SUS304 sheet metals with the thickness of 0.1 mm were utilized as the testing material. To obtain different grain sizes, the specimens were heat treated at different conditions by using an VLT-1200 vacuum tube furnace under argon atmosphere. The furnace was firstly evacuated by using a vacuum pump, and then argon was injected to remove air and served as protective atmosphere. The heating rate during the annealing process was set as 10 ℃/min, and four annealing temperatures were selected as 900, 950, 1000, 1050 ℃, respectively. When reached the target temperature, the temperature was kept at the target value for 15 mins. Finally, the specimens were furnace cooled to room temperature.

After heat treatment, the microstructures of the grain sizes of the specimens are observed by using an optical microscope as shown in Fig. 1. At the annealing temperatures of 900, 950, 1000, and 1050 °C, the grain sizes of the specimens are measured as 22 ± 2, 30 ± 2, 52 ± 4, and 62 ± 6 μm, respectively. Generally, we can see that the grain sizes of the specimen increased as the increasing of annealing temperature. The average number of grains in the thickness

direction decreased as the increasing of annealing temperature. The average number of grains along the thickness of the thin sheet will affect the mechanical properties of materials [23].

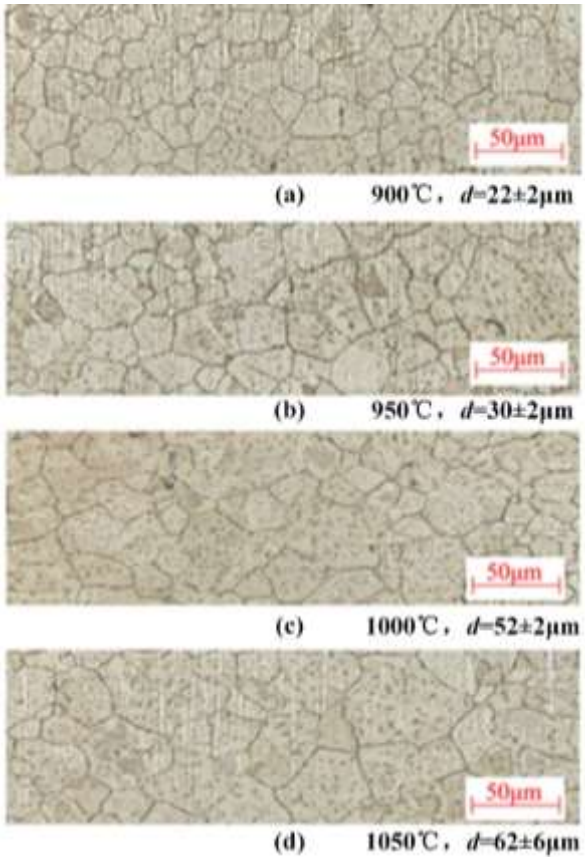

Fig. 1 Microstructures of the specimens at different heat treatment temperatures: (a) 900 °C, *d* = 22 μm; (b) 950 °C, *d* = 30 μm; (c) 1000 °C, *d* = 52 μm; (d) 1050 °C, *d* = 62 μm

2.2 Tensile Testing

Because the specimens occurred plastic deformation during the microstamping process, it is necessary to obtain the strain versus stress relationship for further analysis. Following the standard ASTM-E8 [24], the tensile testing specimens were prepared and their geometric dimensions are illustrated in Fig. 2. The thicknesses of these specimens are 0.1 mm. The uniaxial tensile testing experiments were conducted on a INSTRON5966 material testing machine, a laser extensometer was used to measure the deformation of gauge length. The compression velocity was set as 1.0 mm/min to eliminate the influence of forming speed on the formability. For each specimen, three repeated tests were performed.

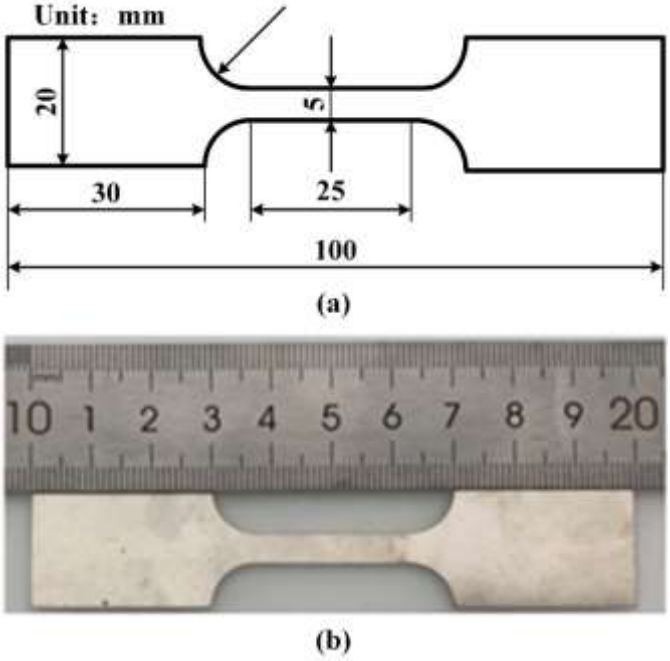

Fig. 2 (a) Design dimension of tensile test specimen; (b) physical tensile test specimen

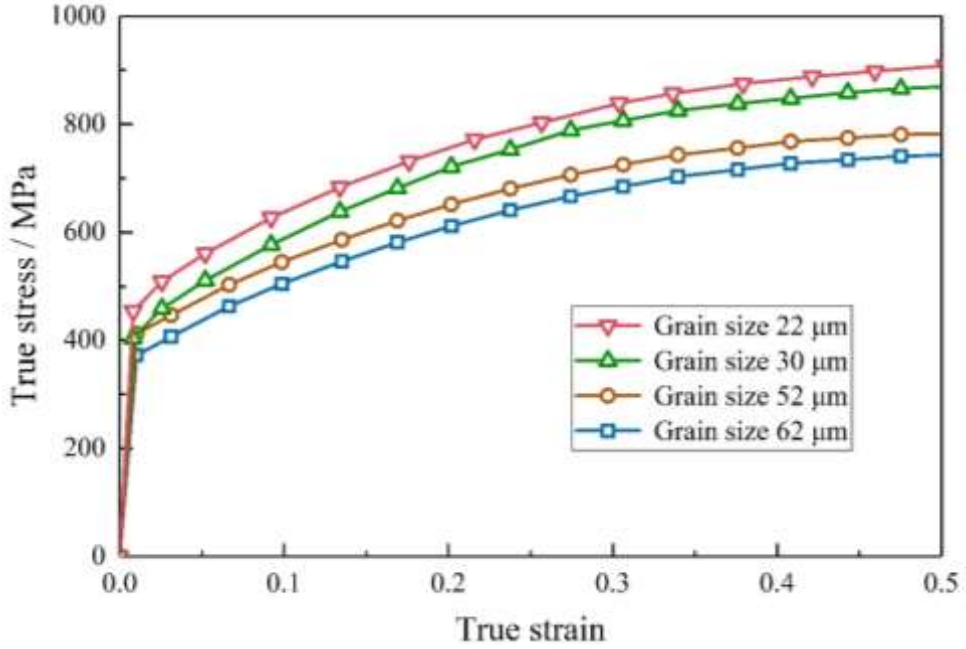

Fig. 3 True stress-true strain curve of SUS304 stainless steel with different grain size

The true stress-strain curves for the specimens with different grain sizes were measured and plotted in Fig. 3. Generally, the measured true stresses increased as the increasing of applied true strain on the specimen. As the grain sizes increasing, the true stress is decreased for the specimen under the same tensile testing conditions. This phenomenon is almost consistent with Hall-Petch equation: the yield strength of the material has almost linear relationship with the reciprocal of the square of grain size. Therefore, the yield strength of the

thin sheet material decreases with the increasing of grain size.

3 Numerical Modelling and Simulation

3.1 Modeling of Constitutive Behavior

To characterize the plastic deformation behavior of thin sheet of stainless steel with different gran sizes, a constitutive model needs to be developed. Prior studies have indicated that the grain boundary has greater strain hardening effects than that of inner grains. Herein, we proposed a geometric model to represent the grains, it can divide the grain structure into two portions: grain inner and grain boundary, as in Fig. 4(a). The regular-shaped hexagons are used to simulate the grain's inner structure, they are evenly wrapped by the grain boundaries. As in Fig. 4(b), we take d to represent the grain size. To study the grain inner and boundary effects, a hybrid constitutive model is proposed to calculate the flow stress of single grain

$$\sigma_s = \lambda_{GI}\sigma_{GI} + \lambda_{GB}\sigma_{GB} \tag{1}$$

$$\lambda_{GI} = \frac{S_{GI}}{S} \frac{\frac{3\sqrt{3}}{2}\left(\frac{d}{2} - \frac{2}{\sqrt{3}}t_B\right)^2}{\frac{3\sqrt{3}}{2}\left(\frac{d}{2}\right)^2} = \left(1 - \frac{2}{\sqrt{3}} \cdot \frac{2t_B}{d}\right)^2 \tag{2}$$

$$\lambda_{GB} = \frac{S_{GB}}{S} = \frac{\frac{3\sqrt{3}}{2}\left(\frac{d}{2}\right)^2 - \frac{3\sqrt{3}}{2}\left(\frac{d}{2} - \frac{2}{\sqrt{3}}t_B\right)^2}{\frac{3\sqrt{3}}{2}\left(\frac{d}{2}\right)^2} = \frac{4}{\sqrt{3}} \cdot \frac{2t_B}{d}\left(1 - \frac{1}{\sqrt{3}} \cdot \frac{2t_B}{d}\right) \tag{3}$$

where σ_{GI} and σ_{GB} are the flow stress of grain inner and grain boundary; λ_{GI} and λ_{GB} represent the area proportions of grain inner and grain boundary, S_{GI} and S_{GB} are the area of grain inner and grain boundary, S is the area of grain; t_B is the thickness of grain boundary.

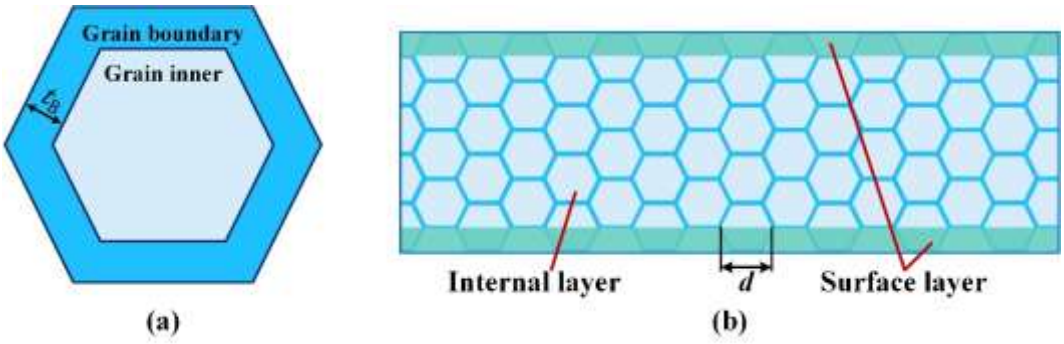

Fig.4 (a) microstructure of grain and (b) surface layer model

Therefore, the flow stress for single grain can be expressed as [25]

$$\sigma_s = \sigma_{GI} + \left(\frac{8t_B}{\sqrt{3}d} - \frac{16t_B^2}{3d^2} \right) (\sigma_{GB} - \sigma_{GI}) \tag{4}$$

The above equation describes the flow stress of single grain considering the grain boundary. For the whole thin sheet material, it can also be divided into two portions: internal layer and surface layer, as shown in Fig. 4 (b). Therefore, the stress of material can be expressed as the weighted average of the stresses in inner portion and surface layer of the specimen as

$$\sigma = (1-\eta)\sigma_{surf} + \eta\sigma_{inner} \tag{5}$$

$$\eta = \frac{t - 2 \cdot \frac{\sqrt{3}}{4} d}{t} = \frac{2t - \sqrt{3}d}{2t} \tag{6}$$

where σ_{surf} and σ_{inner} are the flow stress of surface grains and internal grains; η is the size factor evaluating the portion of internal grains; τ_R is the single crystal's critical resolved shear stress.

Due to the free surfaces, the surface grains are less restricted and their properties can be described by single crystal material. Due to the grain boundaries, the internal grains can be assumed to be polycrystalline material [27], thus the σ_{surf} and σ_{inner} can be expressed as

$$\sigma_{surf}(\varepsilon) = m\tau_R(\varepsilon) \tag{7}$$

$$\sigma_{inner}(\varepsilon) = M\tau_R(\varepsilon) + \frac{k(\varepsilon)}{\sqrt{d}} \tag{8}$$

$$\begin{cases} m\tau_R(\varepsilon) = \mathrm{k}_0\varepsilon^{n_0} \\ M\tau_R(\varepsilon) + \dfrac{k(\varepsilon)}{\sqrt{d}} = \mathrm{k}_1\varepsilon^{n_1} + c_1 \end{cases} \tag{9}$$

where $m$is the reciprocal of the Schmid factor; M is an orientation related factor in polycrystalline material [26]; k is the grain boundary locally intensified stress. Substituting Eqs. (7)-(9) into Eq. (5), the flow stress can be rewritten as

$$\sigma = \mathrm{k}_0\varepsilon^{n_0} + \eta\left(\mathrm{k}_1\varepsilon^{n_1} + c_1 - \mathrm{k}_0\varepsilon^{n_0}\right) \tag{10}$$

According to the previous description, the grains of the inner layer have grain boundaries. Therefore, the flow stress of the internal grains can also be represented by σ_s in Eq. (4). Besides, there are no grain boundaries in the surface layer grains. So, the flow stress of the surface layer

can be represented by the σ_{GI}. Therefore, the flow stress can be expressed as

$$\sigma = \sigma_{GI} + \eta\left(0.614d^{-0.3} - 0.094d^{-0.6}\right)\left(\sigma_{GB} - \sigma_{Gl}\right) \tag{11}$$

It can be found that Eq. (10) has the same form as Eq. (11). Therefore, the following relationship can be obtained

$$\begin{cases} \sigma_{GI} = \mathrm{k}_0\varepsilon^{n_0} \\ \left(0.614\mathrm{d}^{-0.3} - 0.094\mathrm{d}^{-0.6}\right)\left(\sigma_{GB} - \sigma_{GI}\right) = \mathrm{k}_1\varepsilon^{n_1} + c_1 - \mathrm{k}_0\varepsilon^{n_0} \end{cases} \tag{12}$$

Based on the measured strain-stress curves obtained from tensile tests, the parameters (k_0, n_0, k_1, n_1, c_1) can be determined using least square fitting and results are listed in Table 1. These parameters were employed to calculate the flow stress and the stress-strain curves of grain boundary and grain inner of different grain sizes, the results are shown in Fig. 5(a). Due to the higher dislocation densities, grain boundary has higher work-hardening rate, thus leads to greater flow stress compared to that of grain inner. Therefore, the flow stress of grain boundary is significantly larger than the flow stress of grain inner as shown in Fig. 5(a). In addition, as the grain size increases, the flow stress of the grain boundary increases. However, the overall flow stress of the material decreases as the grain size also increases. This is because as the grain size increases, the number of grains in the thickness direction of thin sheet metal decreased, resulting in an increase in the number of grains in surface layer. The inner grains require greater flow stress to maintain the flow stress of the whole material. As a result, the flow stress of the grain boundary increases with the increasing of grain size.

Table 1 The fitted parameters for constitutive model

Grain size/μm	k_0/MPa	n_0	k_1/MPa	n_1	c_1/MPa
22	111.28	0.2359	843.23	0.2885	290.13
30	56.677	0.0011	1029.7	0.3048	294.72
52	230.57	4.5E-6	1268.7	0.3424	257.81
62	222.52	5.5E-6	1465.0	0.4010	280.21

According to the fitted stress-strain curves of the grain boundary and grain inner in Fig. 5(a), the flow stress of thin sheet material was calculated and plotted as shown in Fig. 5(b). It can be observed that the true stress calculated by the developed constitutive model shows a good agreement with experimental results. Therefore, our developed constitutive model can be used to study the deformation behavior of thin sheet material in multi-channel microstamping process.

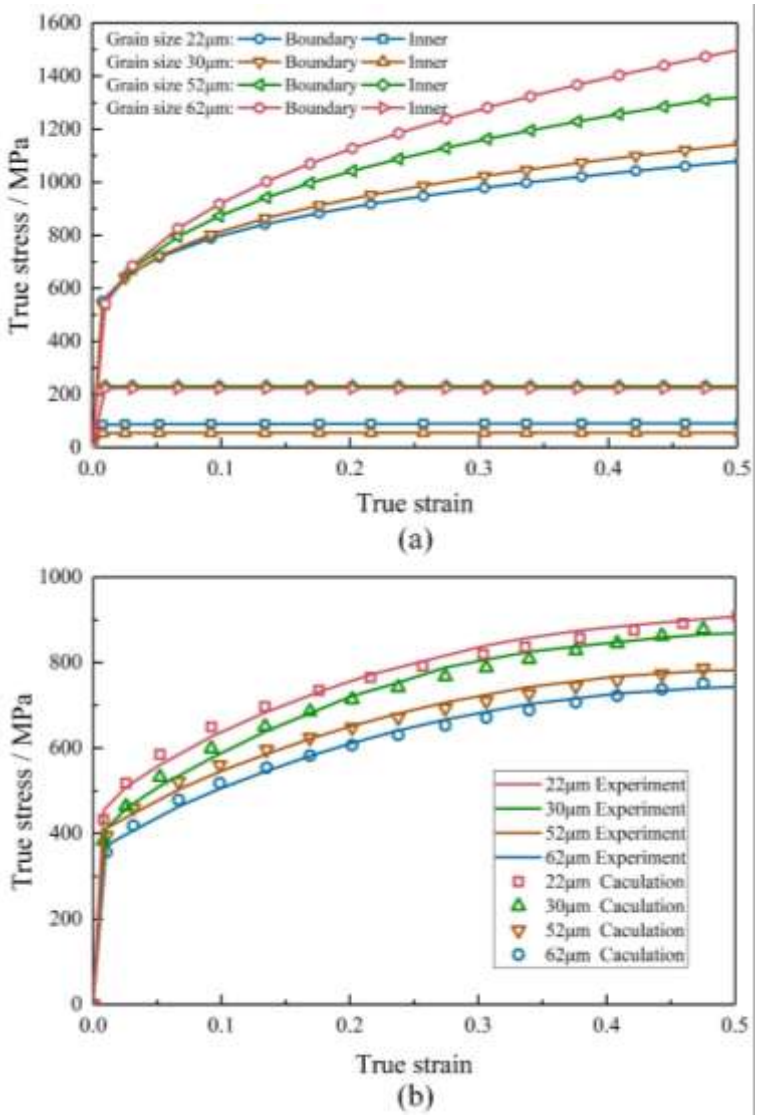

Fig. 5(a) Comparison of experimental and fitted results and (b)True stress-true strain curves for grain boundary and grain inner

3.2 Finite Element Modeling of Multichannels Microstamping

To study the deformation behavior of thin sheet material for the stamping of microchannels, finite element (FE) simulation was performed using the software of Abaqus v.2020. In Fig. 6(a), considering the efficiency of Voronoi tessellation, a 2D axisymmetric geometric specimen with dimensions of 9.0 mm in length and 0.1 mm in thickness was built. Top is the punch and bottom are the die structure, the ridge widths and clearances of the punch and die were set as 0.7 mm and 0.3 mm, respectively. The fillet radii of the punch and die were set as 0.2 mm. The friction between the thin sheet and punch and die was set as 0.1. The material properties of thin sheet material with different grain sizes were set according to the stress-strain curves of the grain boundary and grain inner, which can be obtained as in Fig. 5(a). Three

channels were used in the simulation, and the six-channel micro-stamping process can be simulated through symmetrical boundary conditions, which is enough to verify the performance of the model. During the simulation, the microstamping speed of the punch was set as 1.0 mm/min, and the die was set fixed. The punch and die are regarded as rigid bodies, there was no need for element meshing. For element meshing, CPE4R element was selected and applied to model the thin sheet material. Totally ten elements along thickness direction was modeled to ensure the accuracy of the model.

For the comparison, a microstamping simulation without using our developed constitutive model was set up as shown in Fig. 6(b) to verify the accuracy of FEM simulation results. The material properties of FEM model were set according to the measured stress-strain curves of thin sheet material obtained in Fig. 3.

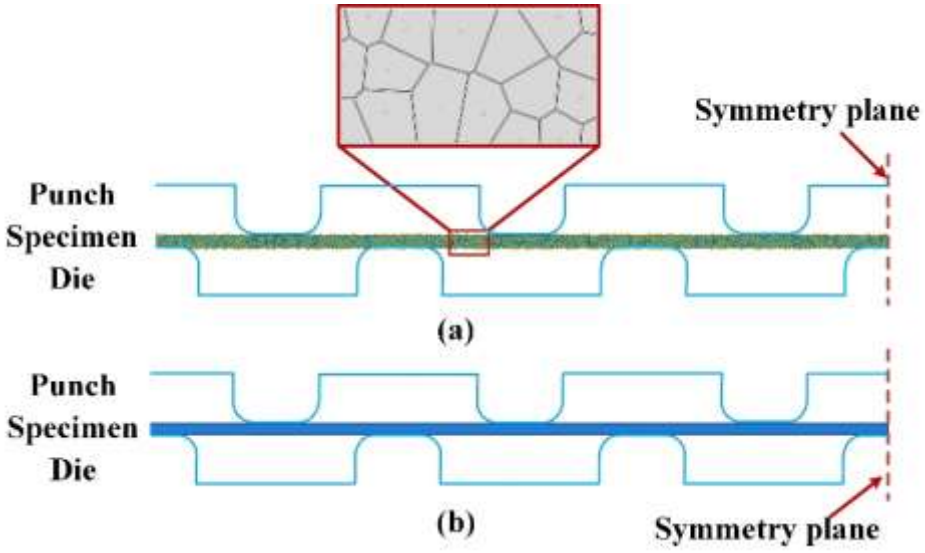

Fig. 6 FE modelling of multichannel microstamping: (a) considering grain boundary structure, (b) not considering grain boundary structure

4 Microstamping Experiment Setup and Procedure

In order to test the multi-channel microstamping performance of SUS 304 specimens with different grain sizes, we designed and fabricated a microstamping die. The dimensions of the punch and die including H_x, fillet radius (R_x), clearance (C_x), and channel width (W_x), are shown in Fig. 7(a). The specimens with the dimension of 18 mm in length, 10 mm in width, and 0.1 mm in thickness are fabricated in the method presented in Section 2.1.

The punch and die were respectively installed on the mold base, both of them were

positioned with pins and fixed with bolts. The springs were installed on the four guide posts, and then the punch and die bases were closed to complete the mold assembly, as shown in Fig. 7(d). The multi-channel microstamping experiments were carried out on an INSTRON5966 material testing machine. A high-resolution industrial camera (Lumenera INFINITY-3) with five mega pixels was used to record the deformation behavior of thin sheets during microstamping process with frequency of 1.0 frame/s. The assembled mold was installed on the material testing machine, and the industrial camera was fixed with a tripod, as shown in Fig. 7(d). Repeatedly adjust the height and position of the camera to clearly observe the forming process.

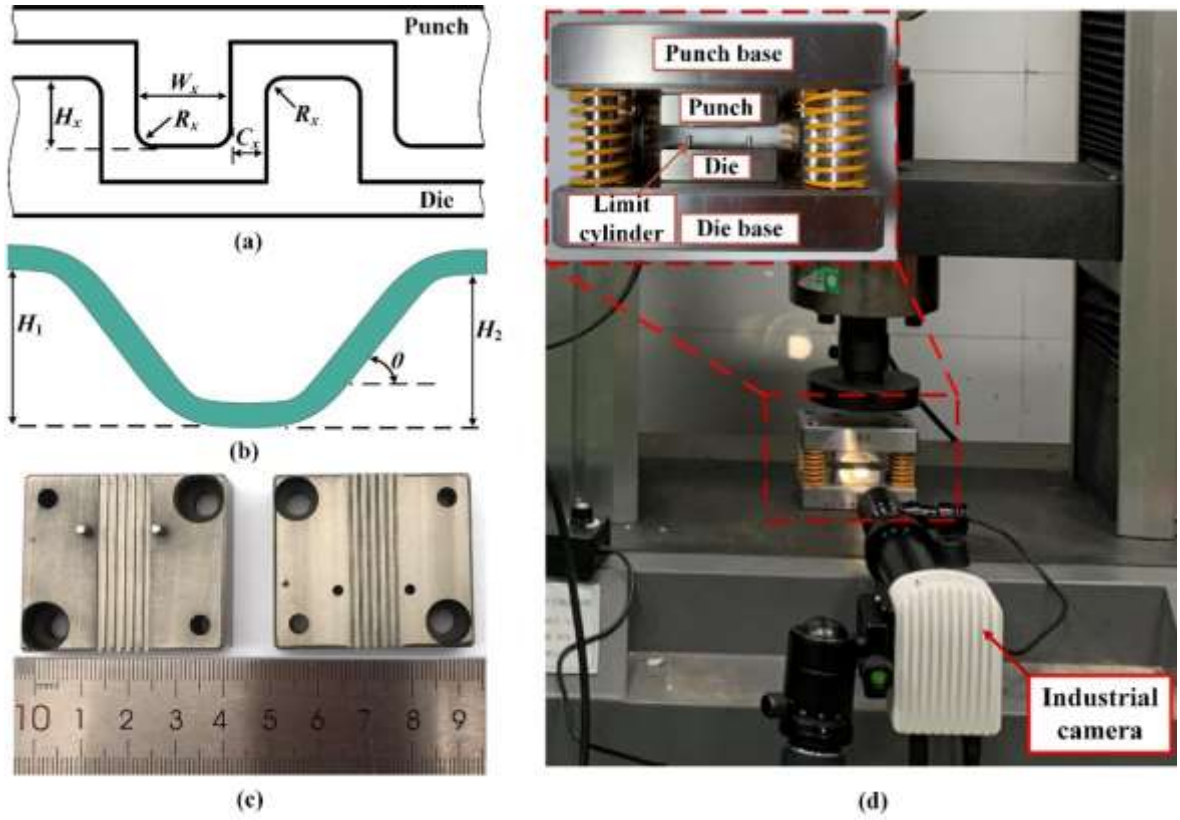

Fig. 7 Schematic of the processing parameters and punch/die apparatus for microstamping experiment: a) definitions of the parameters; b) measurement of the indicators; c) the fabricated punch and die; d) microstamping setup

Use the adjusted experimental system to carry out the micro-channel forming experiment, and the micro-channel forming depth was set to 0.4 mm. The specimen was placed on the die, and the punch was moved down by using the material testing machine until the punch touched the specimen. The moving speed of the punch was set at 1mm/min and the multi-channel microstamping experiment began. After the channels of specimen were stamped to the pre-

determined depth, the punch was held for 120 seconds and then returned at the same speed. Three tests were carried out on the thin sheets of each grain size to verify the accuracy and repeatability of the experiment.

The forming depth (H) and draft angle (θ) of stamping channels are selected as indicators for evaluating the qualities of microchannels in microstamping process, as shown in Fig. 7(b). Based on both two indicators, we can study the springback behavior of each channel after microstamping process. Further, the influences of size effects on microchannels stamping process can be analyzed.

5 Results and Discussion

5.1 Model Verification

In order to verify the model accuracy, microstamping experiments using the specimens with grain size of 52 μm are conducted. The simulation and experimental results of the multi-channel microstamping are shown in Fig. 9. It can be observed that the maximum forming depth in the simulation with and without considering grain boundary is 0.41 mm and 0.38 mm, respectively. The experimental measured maximum forming depth is about 0.40 mm, only about 2.5% lower than that of the simulation considering grain boundary. The shape of third channel (in red dashed line frame) is displayed in detail. The forming depth and draft angle of the simulations with and without considering grain boundary are 0.379 mm, 35.27° and 0.368 mm and 32.49°, respectively. The experimental results of multichannel microstamping showed that the forming depth and draft angle are about 0.378 mm and 37.08°, respectively, as in Fig. 9. Thus, we can conclude that the channel's shape of the simulation results considering the grain boundary is more accurate and consistent with experimental results.

The simulation and experimental forming depth and draft angle results of three channel are illustrated as in Fig. 10. The channel depth decreases continuously from the edge channel (0.393 mm) to the middle channel (0.378 mm), the draft angle decreased from 42.69° to 37.08°. The springback behavior of the channel can be divided into two categories: the springback in the fillet area and the springback in the sidewall area. The springback in the fillet area has the same effect on the edge and central channels. During microstamping process, the fillet area of the channel was subjected to tensile stress and bending stress. The fillet area shrinks, resulting

in a decrease in the forming depth and the draft angle during the springback process. For the springback in the sidewall area, the impact on the middle channel and the edge channel is different. For the central channel, the effect of the drawbead in the sidewall area is more obvious, and it is subject to larger tension stress. Since the effect of the tension stress is larger than the effect of the bending stress, the sidewall area is mainly in a stretched state. After the punch was unloaded, the springback behavior occurred in the sidewall area in the stretching direction, resulting in the decreasing of the forming depth. For the edge channel, the tensile force on the sidewall area is small. The effect of the bending stress is larger than the tensile stress effect, and the sidewall area mainly presents a bending state. After the punch was unloaded, the springback behavior of the sidewall area was not obvious. Therefore, the springback behavior of the central channel includes the springback of the fillet area and sidewall area, while the springback behavior of the edge channel is mainly the springback of the fillet area. As a result, the center channel has greater springback behavior, resulting in a smaller forming depth and draft angle.

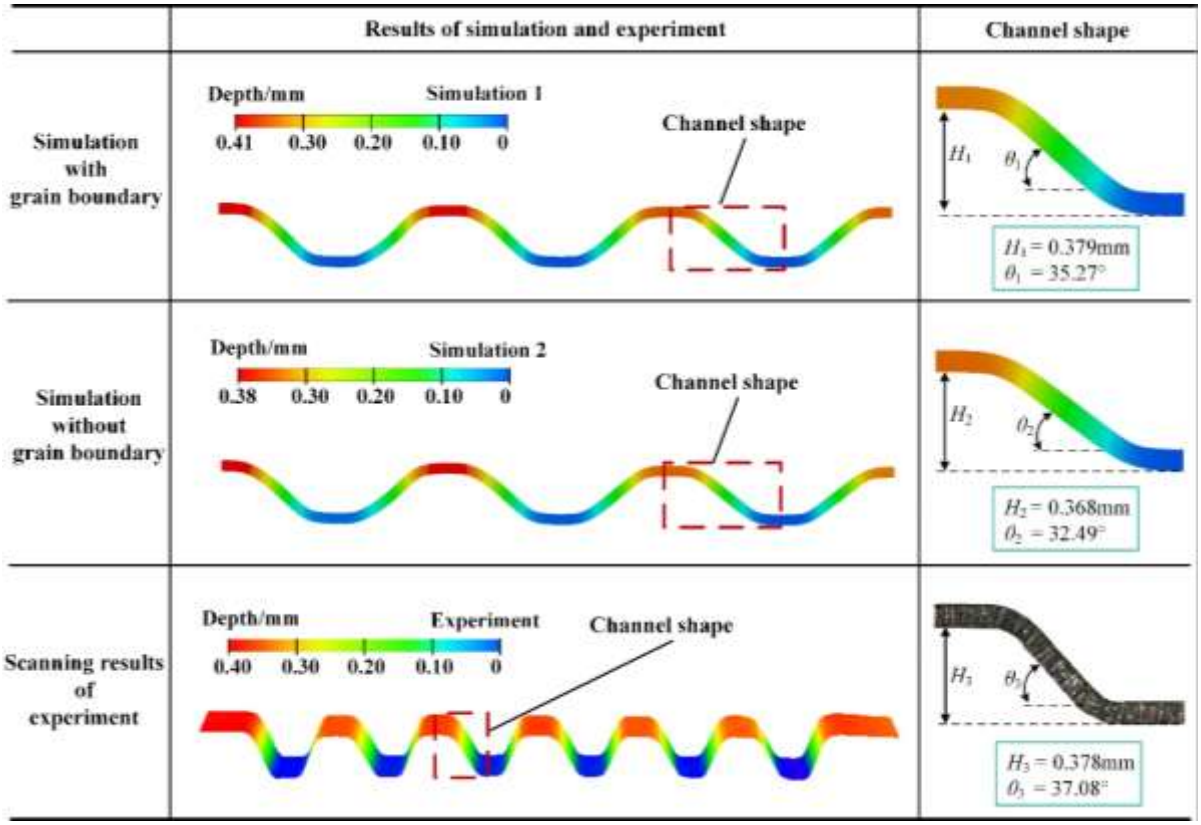

Fig. 9 Simulation and experimental results of multichannel microstamping

From the simulation and experimental results, the simulation results considering grain

boundary is more accurate. The maximum forming depth and draft angle deviation between the experimental and simulation considering grain boundary is 0.6 % and 4.9 %. Besides, the simulation results not considering grain boundary structure are smaller, indicating that it tends to overestimate the springback behavior. This is because the flow stress of the internal grains is greater than the surface grains due to the grain boundary structure of the internal grains. In addition, the surface grains are subjected to stronger tensile and compressive stresses since the surface grains are further from the neutral layer in the micro-stamping experiment. Therefore, the surface grains are more prone to plastic deformation and have a more significant impact on the springback behavior of the material. As a result, the simulation results considering grain boundary structure would have greater plastic strains.

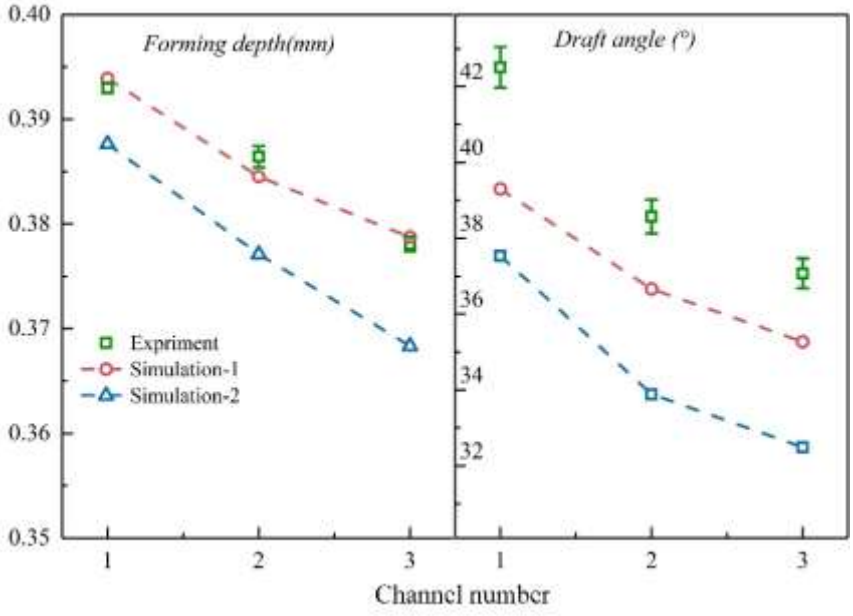

Fig. 10 Comparison of indicators results between experiments and simulation (d = 52 μm)

5.2 Simulation Results of Multichannel Microstamping

The micro-stamping process and the Y-displacement distribution over time are shown in Fig. 11. The specimen was punched at the speed of 1mm/min for 0.4 min and then the force is kept for 2 min. The punch risen at the same speed after remaining in this position. As shown in Fig. 11, when the punch was unloaded, the Y-displacement of the specimen was reduced from 0.404 mm to 0.358 mm, indicating that the specimen has a springback behavior. In addition, it can be observed that the maximum forming depth occurs at the edge channel.

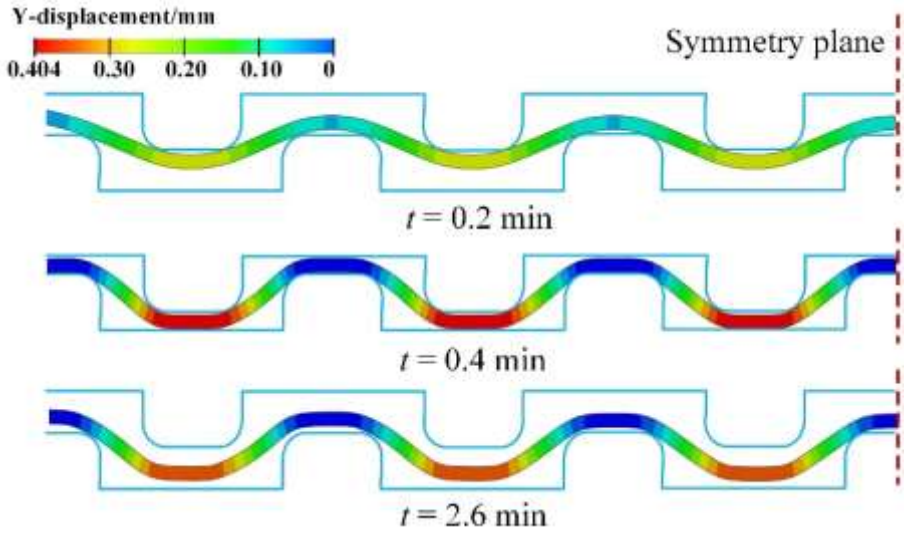

Fig. 11 Multichannel microstamping process at different time

Fig. 12 shows the von mises stress distribution of the specimen with the grain size of 30 μm. It can be seen that the von mises stress at the fillet is 960 MPa, the von mises stress in the middle of the channel is 500 MPa, and the von mises stress on the sidewall of the channel is 200 MPa. The fillet area has stronger von mises stress during the micro-stamping process due to the stronger compressive and tensile stresses. Therefore, the fillet area is the area where the thickness decreases the fastest during the micro-stamping process. In the central part of each flow channel, there is an area has smaller von mises stress. This is because the contact between the specimen and the punch is mainly concentrated near the fillet area, and the central part of the flow channel farther from the fillet area suffers less tensile and compressive stress. In addition, the area with lower von mises stress is close to the neutral layer, which also reduces the tensile and compressive stress in this area. Besides, the von mises stress in grain boundary (960 MPa) is stronger than that grain inner (700 MPa). Obvious stress concentration occurs at the grain boundaries in microstamping process and can be explained by Taylor's formula [26,28]:

$$\sigma = M\alpha b\mu\sqrt{\rho} \tag{13}$$

where M is the Taylor factor; α is a constant; b is the Berdov vector; μ is the shear modulus; and ρ is the dislocation density. According to Taylor's relationship, the flow stress of material is proportional to the square root of the dislocation density. In the process of plastic deformation of the thin plate material, dislocations are continuously generated in the grains and

transferred to the surroundings. Then dislocations accumulate at the grain boundaries, resulting in a large dislocation density. Therefore, the flow stress at the grain boundaries is stronger than that at the grain inner. In addition, the grain boundary presents a highly rigid network structure, which leads to stress concentration and prevents the occurrence of deformation.

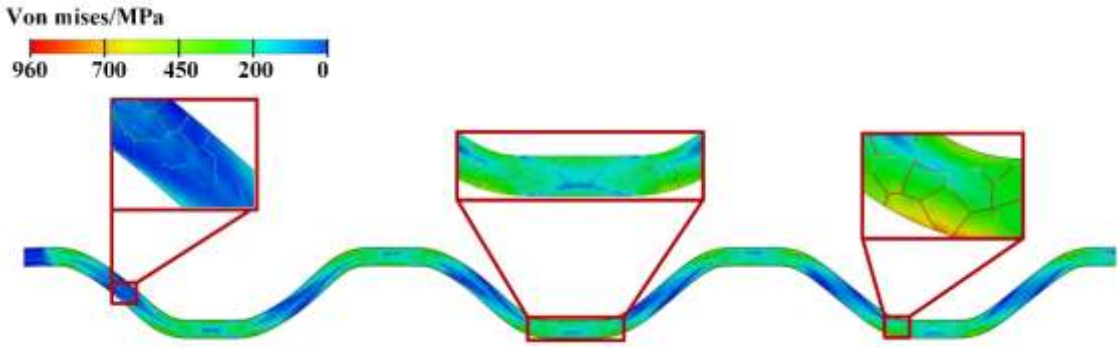

Fig. 12 Distribution of von mises stress in multichannel stamping (d = 30 μm)

Different from the distribution of von mises stress, plastic strain is mainly concentrated in grains inner, and almost no plastic strain occurs at the grain boundaries. The plastic strain distribution of different channels and different grains after micro-stamping is shown in Fig. 13(a). The plastic strain at the fillet is 0.18, the plastic strain in the middle of the channel is 0.1, and the plastic strain on the side wall of the channel is almost 0. Consistent with the distribution of von mise stress, the plastic strain of the fillet area is higher than other positions indicating that the fillet area is most prone to fracture. This is because that compare with the grains inner, the formation of the grain boundaries is more difficult. Due to the irregular arrangement of atoms and the severe distortion of the grain boundary lattice, the dislocation slip of the grain boundary is limited. To coordinate the plastic strain of the grains inner with the plastic strain of the grain boundary, more slip systems are required. Therefore, the deformation of grains inner is much easier than the grain boundary.

The plastic strain distribution of different grain sizes is shown in Fig. 13(b)-(e). As the grain size increases from 22 μm to 62 μm, the maximum plastic strain of the runner increases from 0.16 to 0.21. This is because as the grain size increases, the proportion of grain boundaries decreases and plastic strain occurs and the springback behavior becomes more obvious. The forming depth of the channel increases with the increase of the grains size. For specimens with smaller grain size, the maximum plastic strain in the fillet area of the channel is mainly

concentrated at the junction between the grains inner and the grains boundary. For specimens with greater grain size, the maximum plastic strain is mainly concentrated on the grains inner. Therefore, specimens with larger grain sizes may occur transgranular fracture, while the fracture of specimens with smaller grain sizes may occur at the junction of grains inner and grain boundaries.

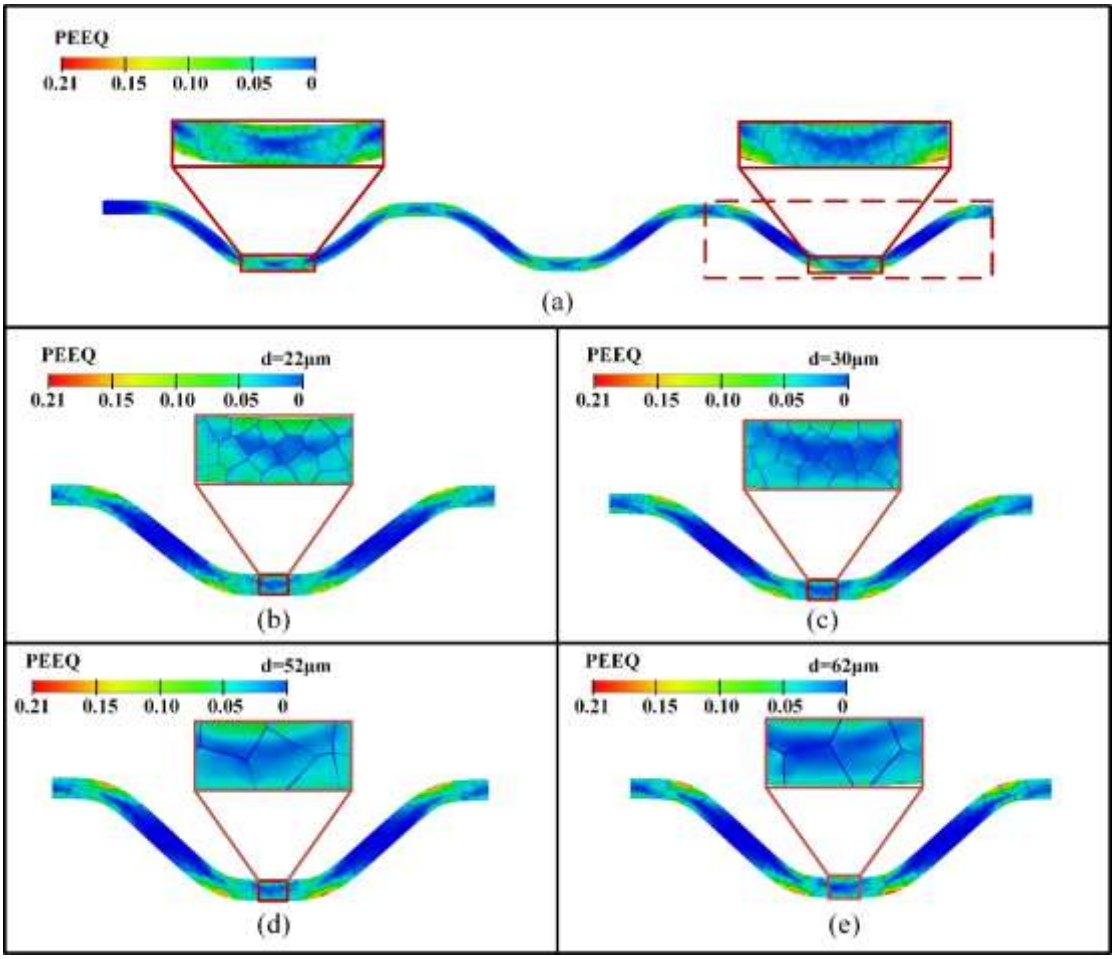

Fig. 13 Plastic strain distribution for different channels and different grain sizes: (a) *d* = 30 μm; (b)~(e) plastic strain distribution of different grain size (channel in the dashed frame in (a))

5.3 Experiment Results

Specimens with grain sizes of 22, 30, 52, and 62 μm were formed into 6 channels after microstamping experiment, as shown in Fig. 14 (a)-(d). The forming depth and draft angle of each channel of the specimens after experiment were measured using Olympus confocal laser scanning microscope (OLS-4100). The forming depth and draft angle of different channels are shown in Fig. 15. As the grain size increases from 22 μm to 62 μm, the channel depth rose from 0.364 mm to 0.389 mm. In addition, the depth's differences between the edge channel

and central channel decreases from 0.018 mm to 0.01 mm, as the grain size increases from 22 μm to 62 μm. It shows that the springback behavior tends to decrease with the increase of grain size. Therefore, to obtain a deeper and more uniform flow channel depth, the thin sheet specimen with larger grain size should be used.

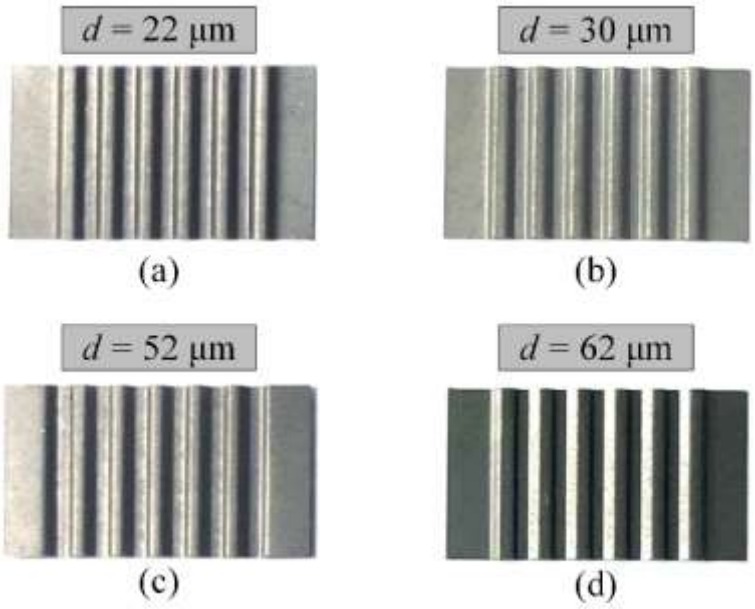

Fig. 14 Specimens after multichannel microstamping experiment

Similar to the forming depth, the draft angle of the channels also increases with the increasing of grain sizes, as shown in Fig. 15(b). As the grain size increases from 22 μm to 62 μm, the draft angle increased from 35.94° to 39.78°. The draft angle is an important indicator that determines the channel shape and describes the size of the springback behavior. As a result, channel with larger draft angle can be obtained with larger grain size specimens. As the grain size increases, the springback behavior of the specimen is reduced. This is because the specimens with larger grain size have smaller flow stress, resulting in insignificant elastic recovery. As a result, the specimens with larger grain size are more prone to plastic deformation under the same deformation conditions. As the grain size increases, the number of grains in the thickness direction of the sheet decreases, resulting in an increase in the proportion of surface layer grains. The flow stress of the surface layer grains is smaller than that of the internal grains. Therefore, as the proportion of surface layer grains increases, the specimens occur more plastic deformation and the springback tendency decreases.

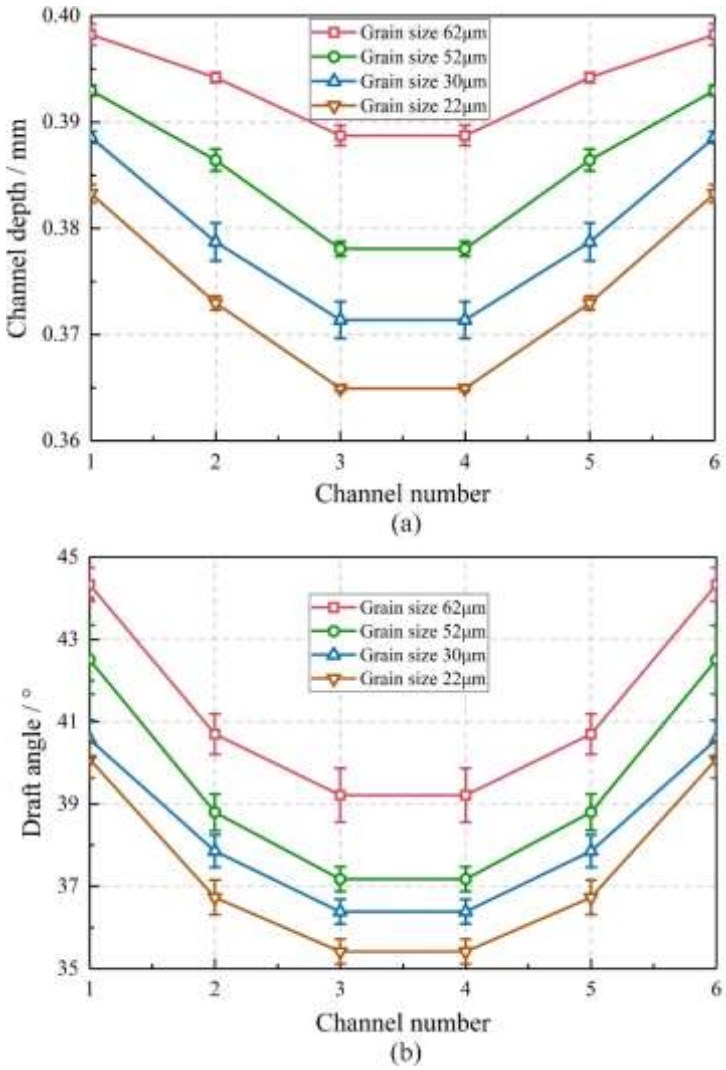

Fig. 15 Evolution of the indicators with decreasing grain size: a) forming depth and b) draft angle

6 Conclusions

This paper developed a constitutive model considering surface layer and grain boundary to investigate the springback behavior of SUS304 thin sheets for multichannel microstamping. The proposed model accurately predicted the forming depth and draft angle in multichannel microstamping process with low errors of 2.5% and 4.9%, respectively. Through experiments and FE simulation analysis, it was observed that the channel depth decreased by 3.8% from the edge to central channels. And the reason was analyzed from the stress in each area of the channel during the stamping process. Experimental and simulation results showed that increasing the grain size can suppress the springback phenomenon. When the grain size increased from 22 μm to 62 μm, the channel depth and draft angle was increased by 6.4% and

9.6%, respectively.

In order to improve the dimensional accuracy of the fabricated microchannels, future work will focus on controlling the springback through the compensation method. And the microstamping experiments to fabricate complicate channel structures will be guided by the developed constitutive model.

Author contribution All authors contributed to the study conception and design. Material preparation, data collection and analysis were performed by Shangyu Si, Qiong Wu and Wenze Mao. The first draft of the manuscript was written by Shangyu Si and all authors commented on previous versions of the manuscript. All authors read and approved the final manuscript.

Funding The authors acknowledge the financial support from the National Natural Science Foundation of China (U1809220), Key Research and Development Program of Zhejiang Province (2022C01113).

Availability of data and materials All data generated or analyzed during this study are included in this submitted article.

Declarations

Competing Interests The authors have no relevant financial or non-financial interests to disclose.

Ethics approval Not applicable.

Consent to participate Not applicable.

Consent for publication Yes.

Consent for publication The authors have consented to publish the research article in the journal.

References

[1] R. Ruprecht, T. Gietzelt, K. Muller, V. Piotter, J. Hausselt, Injection molding of microstructured components from plastics, metals and ceramics, Microsystem Technologies 8(4-5) (2002) 351-358.

[2] M. Belali-Owsia, M. Bakhshi-Jooybari, S.J. Hosseinipour, A.H. Gorji, A new process of forming metallic bipolar plates for PEM fuel cell with pin-type pattern, International Journal of Advanced Manufacturing Technology 77(5-8) (2015) 1281-1293.

[3] X.N. Li, S.H. Lan, Z.T. Xu, T.H. Jiang, L.F. Peng, Thin metallic wave-like channel bipolar plates for proton exchange membrane fuel cells: Deformation behavior, formability analysis and process design, Journal of Power Sources 444 (2019).

[4] J.E. Carsley, J. Ning, W.W. Milligan, S.A. Hackney, E.C. Aifantis, A Simple, mixtures-based model for the grain-size dependence of strength in nanophase metals, Nanostructured Materials 5(4) (1995) 441-448.

[5] M.W. Fu, J.L. Wang, A.M. Korsunsky, A review of geometrical and microstructural size effects in micro-scale deformation processing of metallic alloy components, International Journal of Machine Tools & Manufacture 109 (2016) 94-125.

[6] K. Suzuki, Y. Matsuki, K. Masaki, M. Sato, M. Kuroda, Tensile and microbend tests of pure aluminum foils with different thicknesses, Materials Science and Engineering a-Structural Materials Properties Microstructure and Processing 513-14 (2009) 77-82.

[7] J.F. Michel, P. Picart, Size effects on the constitutive behaviour for brass in sheet metal forming, Journal of Materials Processing Technology 141(3) (2003) 439-446.

[8] U. Engel, R. Eckstein, Microforming - from basic research to its realization, Journal of Materials Processing Technology 125 (2002) 35-44.

[9] H.Z. Li, X.H. Dong, Y. Shen, A. Diehl, H. Hagenah, U. Engel, M. Merklein, Size effect on springback behavior due to plastic strain gradient hardening in microbending process of pure aluminum foils, Materials Science and Engineering a-Structural Materials Properties Microstructure and Processing 527(16-17) (2010) 4497-4504.

[10] J.G. Liu, M.W. Fu, J. Lu, W.L. Chan, Influence of size effect on the springback of sheet metal foils in micro-bending, Computational Materials Science 50(9) (2011) 2604-2614.

[11] M. Geiger, M. Kleiner, R. Eckstein, N. Tiesler, U. Engel, Microforming, Cirp Annals-Manufacturing Technology 50(2) (2001) 445-462.

[12] L.F. Peng, F. Liu, J. Ni, X.M. Lai, Size effects in thin sheet metal forming and its elastic-plastic constitutive model, Materials & Design 28(5) (2007) 1731-1736.

[13] L.F. Peng, P.Y. Yi, P. Hu, X.M. Lai, J. Ni, Analysis of the micro/meso scale sheet forming by strain gradient plasticity and its characterization of tool feature size effects, 9th ASME International Manufacturing Science and Engineering Conference (MSEC2014), Univ Michigan, Detroit, MI, 2014.

[14] D.J. Kim, T.W. Ku, B.S. Kang, Finite element analysis of micro-rolling using grain and grain boundary elements, Journal of Materials Processing Technology 130 (2002) 456-461.

[15] Z.T. Xu, L.F. Peng, M.W. Fu, X.M. Lai, Size effect affected formability of sheet metals in

micro/meso scale plastic deformation: Experiment and modeling, International Journal of Plasticity 68 (2015) 34-54.

[16] R. Zhang, Z.T. Xu, L.F. Peng, X.M. Lai, M.W. Fu, Modelling of ultra-thin steel sheet in two-stage tensile deformation considering strain path change and grain size effect and application in multi-stage microforming, International Journal of Machine Tools & Manufacture 164 (2021). 103713

[17] R. Zhang, S.H. Lan, Z.T. Xu, D.K. Qiu, L.F. Peng, Investigation and optimization of the ultra-thin metallic bipolar plate multi-stage forming for proton exchange membrane fuel cell, Journal of Power Sources 484 (2021). 229298

[18] S.G. Xu, K.W. Li, Y. Wei, W.C. Jiang, Numerical investigation of formed residual stresses and the thickness of stainless steel bipolar plate in PEMFC, International Journal of Hydrogen Energy 41(16) (2016) 6855-6863.

[19] C.J. Wang, B. Guo, D.B. Shan, Polycrystalline model for FE-simulation of micro forming processes, Transactions of Nonferrous Metals Society of China 21(6) (2011) 1362-1366.

[20] A. Molotnikov, R. Lapovok, C.F. Gu, C.H.J. Davies, Y. Estrin, Size effects in micro cup drawing, Materials Science and Engineering a-Structural Materials Properties Microstructure and Processing 550 (2012) 312-319.

[21] H.N. Lu, D.B. Wei, Z.Y. Jiang, X.H. Liu, K. Manabe, Modelling of size effects in microforming process with consideration of grained heterogeneity, Computational Materials Science 77 (2013) 44-52.

[22] X. Wang, Q. Qian, Z.B. Shen, J.W. Li, H.F. Zhang, H.X. Liu, Numerical simulation of flexible micro-bending processes with consideration of grain structure, Computational Materials Science 110 (2015) 134-143.

[23] J.L. Wang, M.W. Fu, S.Q. Shi, A.M. Korsunsky, Influence of size effect and plastic strain gradient on the springback behaviour of metallic materials in microbending process, International Journal of Mechanical Sciences 146 (2018) 105-115.

[24] L.F. Peng, P. Hu, X.M. Lai, D.Q. Mei, J. Ni, Investigation of micro/meso sheet soft punch stamping process - simulation and experiments, Materials & Design 30(3) (2009) 783-790.

[25] S. Geibdorfer, U. Engel, M. Geiger, Mesoscopic model - Advanced simulation of microforming processes, 10th ESAFORM Conference on Material Forming, Zaragoza, SPAIN, (2007) 79-84.

[26] X.M. Lai, L.F. Peng, P. Hu, S.H. Lan, J. Ni, Material behavior modelling in micro/meso-scale forming process with considering size/scale effects, Computational Materials Science 43(4) (2008) 1003-1009.

[27] Z.T. Xu, L.F. Peng, E.Z. Bao, Size effect affected springback in micro/meso scale bending process: Experiments and numerical modeling, Journal of Materials Processing Technology 252 (2018) 407-420.

[28] C.W. Sinclair, W.J. Poole, Y. Brechet, A model for the grain size dependent work hardening of copper, Scripta Materialia 55(8) (2006) 739-742.